On the Use of a Janus-like Frame to Estimate the Channel Characteristics in Adaptive Communications

Ananya Battacharya[1] and Jean-Francois Bousquet[1]

[1]Dalhousie University, Electrical and Computer Engineering,

Halifax, Nova Scotia, Canada
ananya@dal.ca, jfbousquet@dal.ca.

Abstract: *The JANUS protocol is typically recommended for discovery of nodes in an underwater communication network because its modulation scheme is robust to the acoustic channel impairments. In this work, it is proposed to use a JANUS-like broadcast message to identify the instantaneous channel impairments at the receiver. This can allow to define the modulation parameters in a reconfigurable physical layer. In this work, the algorithm to estimate the gain, multipath properties and Doppler spread is described using a frame that is compatible to the JANUS standard. The algorithm is demonstrated on simulated data, as well as on measured data for a communication link with a bandwidth of 5000 Hz at 27.5 kHz.*

Keywords: *JANUS protocol, reconfigurable physical layer, multipath, channel estimation.*

1. INTRODUCTION

Underwater acoustic propagation is characterized by high attenuation, multipath propagation, and time-varying Doppler shifts that can significantly impact the performance of communication systems. Because of the unique challenges posed by the underwater channel characteristics, efficient estimation using low overhead on the data transfer is a critical research area in underwater acoustic communication.

A discovery message can be used to obtain channel propagation conditions. This can serve multiple purposes, for example to optimize the physical parameters such as the modulation type, the coding rate, and the transmit power. The channel estimate estimation can also serve to define different parameters in the communication stack, including at the Multiple Access Layer (MAC) to share the resources and the Network layer for routing purposes.

It should be noted that the long latency in the transmission link prevents feeding back the small scale fading characteristics between the transmitter and receiver. Nonetheless, information about the large scale parameters can serve to optimize the communication link parameters.

Over the years, multiple studies have been conducted to develop efficient and accurate techniques to estimate channel conditions for adaptive underwater communication systems. Pioneering work on adaptive communication systems include [1]. In 2014, Wang et al. [2] proposed a channel estimation method based on a time-frequency domain by exploiting the sparsity of the channel impulse response in a joint domain. In 2020, Zhang et al. [3] proposed an adaptive channel discovery technique based on a cooperative approach that used multiple nodes to estimate the channel parameters and adaptively adjust the transmission parameters based on the channel state information (CSI). This technique was successful in enhancing performance in terms of bit error rate and throughput compared to traditional techniques. In [4], Wang et al. explores the use of Gaussian likelihood and constellation aggregation techniques for improving the accuracy of channel estimation in underwater acoustic communication systems.

Although research on channel discovery for adaptive communication systems for underwater acoustic communication has advanced in recent years, there are research gaps such as robustness to harsh environmental factors, signal interference and frequency-dependent channel effects, energy efficiency to support underwater devices that are often deployed in inaccessible and harsh underwater environments without compromising the communication performance, increasing number of nodes in large-scale underwater networks, lack of standardized communication protocols and interfaces, that still needs to be addressed.

In this paper, a technique for the estimation of the various channel impairments including the Doppler spread, delay spread, signal to noise ratio (SNR) and channel gain has been developed. The model is then applied to a JANUS compatible physical layer centered at 27.5 kHz.

In this paper, the model to estimate various figure of merits that are intended to be sent to the nodes is described. These estimated figure of merits ultimately decide the communication link parameters such as the modulation techniques in an adaptive communication system, similarly to the technique described in [5].

This paper is organized as follows: next, in Section 2, a network model that relies on a discovery message to estimate the channel conditions is described; in Section 3, the algorithm to estimate the channel delay spread is described; Section 4 describes the algorithm used to estimate the Doppler shift and Doppler spread in dynamic conditions; finally, Section 5 provides a conclusion.

2. NETWORK DESCRIPTION

2.1. SIMULATION OF PHYSICAL LAYER

In this section, a physical layer model that adopts several of its features from the JANUS standard is described. The JANUS standard was chosen because of its versatility, reliability, robustness to harsh channel conditions, and reduced susceptibility to interference from other sources [6]. Furthermore, the JANUS standard provides interoperability between different underwater communication systems, allowing for easier collaboration and communication between different organizations and equipment.

As shown in Figure 1, the physical layer described in this work is implemented based on a Binary-Frequency Shift Keying (B-FSK) technique that involves switching between two different frequencies to represent digital transformation. A pseudo random sequence with a length of 1024 bits is used as the discovery message for the model. This PN sequence is encoded by a 1/2 rate convolutional encoder and then B-FSK modulated. The modulated bits are hopped [6] over a set of 13 different tonal pairs, each consisting of two frequencies that are spaced evenly over the bandwidth of 5 kHz. In order to avoid any discontinuities, the frequency hopped B-FSK (FH-BFSK) is implemented with a continuous phase modulation. The use of evenly-spaced tonal pairs ensures that the hopping sequence covers the entire frequency band, thereby securing the communication from interference of any kind.

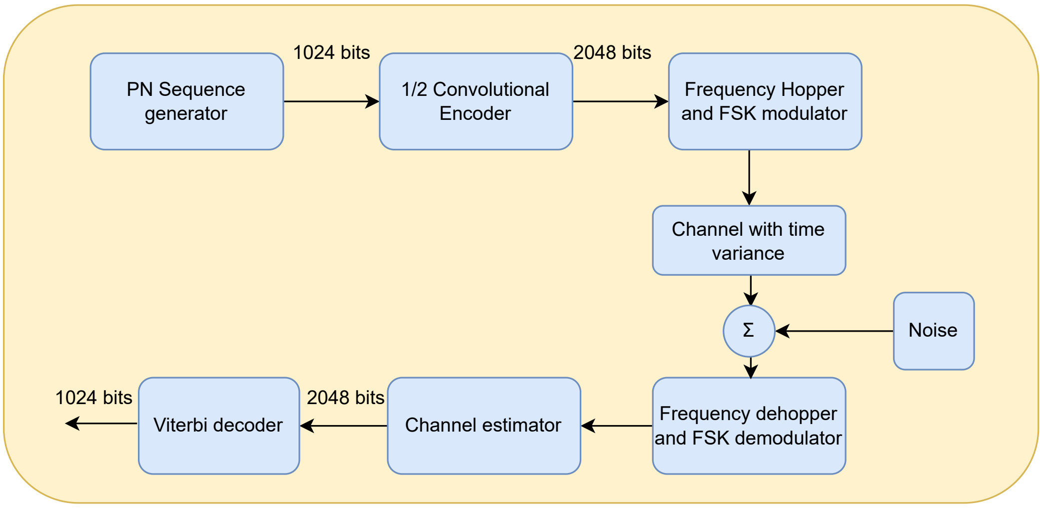

Figure 1: Modelled physical layer of the FH-BFSK system

As shown in Figure 1, the FH-BFSK modulated discovery message is transmitted across a channel with additive white Gaussian noise (AWGN) and an exponentially decaying channel gain.

At the receiver end, the signal is frequency de-hopped, BFSK demodulated and analyzed to estimate the channel conditions. This analysis involves measuring the effects of channel gain, multipath, Doppler shift, and Doppler spread on the signal. A Viterbi decoder is used to recover the 1024 bits of PN sequence.

2.2. REAL-TIME IMPLEMENTATION

The system parameters defining the System-on-Chip implementation are specified in this section. The implementation process is then detailed.

The transmit data frame has a bandwidth of 5 kHz, a frequency of 27.5 kHz, and a length of 1024 bits. The binary baseband frequencies selected for the base-level transmitter are 96 Hz and -96 Hz for binary 1 and 0, respectively. Thirteen symmetrically spaced, pseudo-orthogonal tonal sequences are employed for frequency hopping. Between -2.4 kHz and 2.4 kHz, there is a 384 Hz gap between each of these tones. A 20 millisecond symbol time is defined for transmission in the tank that is expected to suffer from severe multipath. The transmitter was initially modelled on Python and subsequently implemented on VHDL.

The data frame in the transmission chain is generated by a Pseudo-random noise (PN) generator which generates a 1024-bit Gold code at a rate of 20 msec. The Gold code enables the option for a MIMO operation for future enhancements. The Digital Direct Synthesizer (DDS) IP core in Vivado is used for generating the desired complex baseband FSK signal and is sampled at 96 kSps. The DDS is programmed to produce two distinct phase increments to generate the binary frequencies. A bit-to-phase conversion module is defined between the PN generator and the DDS for this purpose. The DDS is fed a 100-MHz clock and a digital complex waveform is obtained at 2.5 kHz. A 1/2 convolutional encoder IP core from AMD/Xilinx is implemented into the system at the output the PN generator and fed to the bit-to-phase converter. Another DDS is used to generate a carrier signal of 27.5 kHz in fixed frequency mode which is then used to upconvert the passband signal to a baseband frequency. Finally, a sigma delta modulation serves to achieve the digital to analog conversion. For the correct pulse density modulation (PDM), the signal must be boosted before entering the pulse density modulator.

To avoid oversaturation in the pulse density modulator, which could lead to challenges with imaging, the signal is multiplied by an integer percentage. The best outcomes were produced by fixing the output signal to approximately 90% of the PDM maximum power. Going higher lead to nonlinearity problems, and going lower might raise the amount of circuit noise. The clock frequency used by the pulse density modulator is 10 MHz. The final signal that is expected from the FPGA comes out of the PDM. It is routed to a board-mounted high-speed port. This signal is delivered to the acoustic source that transmits the underwater acoustic waves after being passed via a low pass filter and power amplifier.

The Aquatron facility at Dalhousie University in Canada served as the testing ground for the transmitter. The transmitter circuit was installed close to the acoustic source, which was submerged to a depth of 2 metres in the pool. A receiver was placed underwater at the other end of the pool.

3. DELAY SPREAD ESTIMATION

The algorithm used to estimate the channel gain is described in this section. First, the received frame is synchronized to the start of the burst and the clock drift is compensated. Then, the received signal $y(t)$ is downconverted using $e^{j2\pi f_c t}$. The residual time-dependent tone for the ith symbol is equal to $f_i = f_i^h + f_i^m$, where f_i^h is the hopping frequency for the ith symbol and f_i^m is the BFSK modulation frequency for the ith symbol. For the ith symbol, to estimate the channel at frequency f_i, first, the signal is multiplied by $e^{-j2\pi f_i t}$. The resulting signal has a DC component, which is integrated over the symbol duration to produce a vector of frequency dependent channel estimates $\hat{\mathbf{H}}_{\mathbf{est}}$, defined as $[f_0, f_1 \cdots f_{M-1}]$ where M is the number of symbols in the frame. To further improve the quality of the channel estimate, the channel estimates at at the 26 discrete known frequencies are averaged to produce a channel frequency response (CFR) $\overline{H_{est}}(f)$.

To assess the channel estimation algorithm, a simulation of the physical layer is run. The transmitted signal is applied to an exponentially decaying multipath channel with unit energy, i.e. $h(\tau) = \exp(-\tau/\alpha)$. The simulation is run for multiple iterations, each time increasing the exponentially decaying factor α; for each run, the RMS delay spread is recorded. After each transmission run, the CFR $\hat{\mathbf{H}}_{\mathbf{est}}(\mathbf{f})$ vector is re-organized to group estimates that belong to the same subcarrier. For example, Figure 2a illustrates the estimated CFR values for a channel with an exponential decay rate of 3. Figure 2 represents the averaged response $\overline{H_{est}}(f)$. As can be observed it is an accurate representation of the actual CFR.

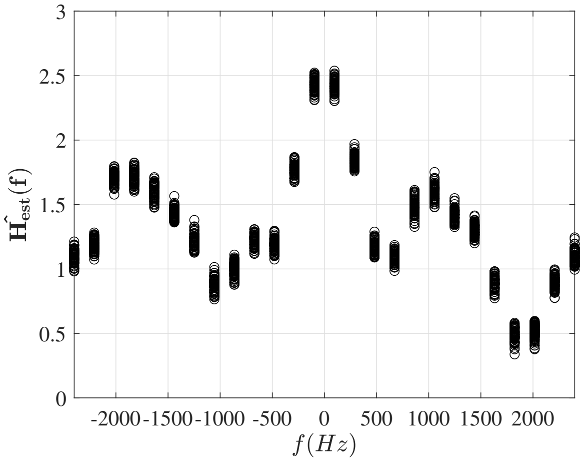

(a) Frequency dependent channel estimates vs. their respective frequencies

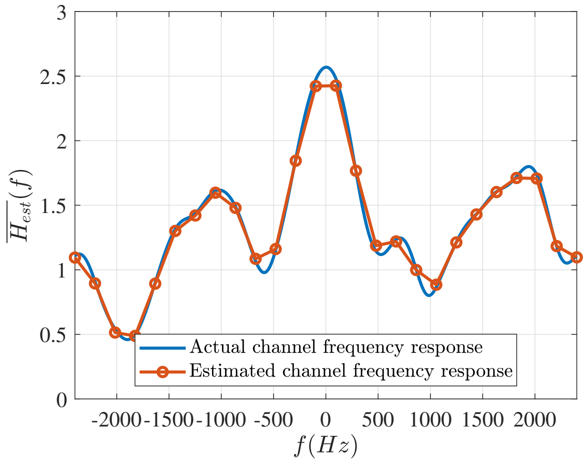

(b) Estimated CFR overlaid with the actual CFR.

Figure 2: Example of an estimated CFR.

To measure the severity of the multipath channel, the statistics of the measured frequency response $\hat{\mathbf{H}}_{\mathbf{est}}(\mathbf{f})$ are calculated. Specifically, the variance for each subcarrier $\sigma^2_{H(f)}$ is calculated. The mean of $\sigma^2_{H(f)}$ μ_{H_f}, and variance of $\sigma^2_{H(f)}$, $\sigma^2_{H_f}$ are calculated across to obtain a single value for a given transmission, and the results are recorded. In simulation, this process is repeated for all 14 decay rates. Given that the model incorporates a random phase in the transmitted signals, the algorithm is executed 100 times to generate an averaged value for the mean, $\overline{\sigma^2_H}$, and variance, $\sigma^2_{\sigma^2_H}$, of the 26 subcarriers across the 14 different channel conditions. To maintain conformity, the RMS delay spread values for each of these channels were simultaneously recorded and averaged over the 100 simulations.

Figure 3 shows the plot for the mean of the variance $\overline{\sigma^2_H}$ and the standard deviation $\sigma_{\sigma^2_H}$ of the variance for the channel estimate plotted against the RMS delay spread. The measured variance and mean values that are recorded during the measurements in the Aquatron are also recorded. The values obtained are representative of an RMS delay spread between 2.5 msec and 2.7 msec.

The mean and variance of an estimated underwater wireless channel provides important information about the expected behavior of the wireless channel. By analyzing the mean and variance values across different channel conditions, a better understanding of the impact of different channel scenarios on the wireless channel, as well as on the channel estimation algorithm itself, was realized. The fact that the variance of the variance increases as the channel gets worse suggests that the variability of the estimated channel values becomes increasingly unpredictable

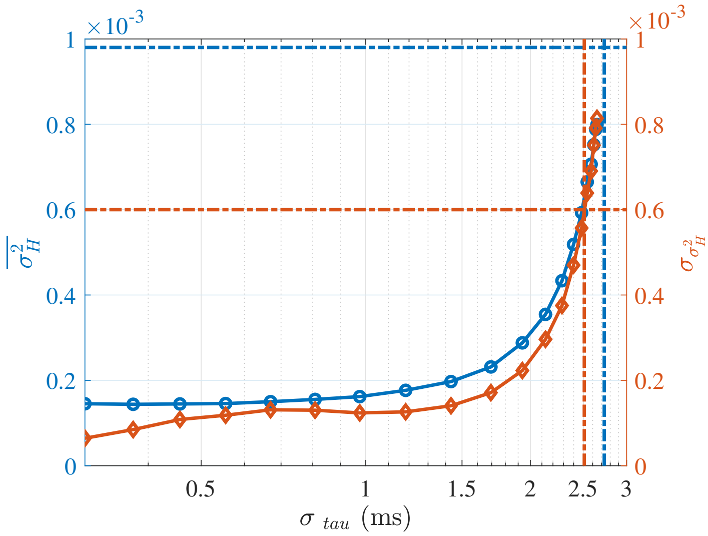

Figure 3: Channel mean and standard deviation against RMS delay spread

and unstable as channel conditions get more challenging. The increasing mean of the variance with worsening channel conditions are indicative that the multipath arrivals create additional noise on each subcarrier.

4. DOPPLER SPREAD ESTIMATION

In this section, how the Janus preamble can be used to extract an estimate of the Doppler shift and Doppler spread is presented.

First, as described in [7], an auto-correlation on the signal is used on the input buffer to get the time scaling factor that induces time dilation and is equal to $\mu = (1 + v/c)$. The signal can then be resampled by a factor $1/\mu$ to compensate for the large scale Doppler.

Then, after downconversion, the received signal is multiplied by the conjugate of the transmit signal, and the Doppler spectrum is obtained using the Welch approximation, which computes the power spectral density by dividing the data into overlapping segments, computing a modified periodogram for each segment and averaging the periodograms.

Using an FFT size $N_{FFT,DS}$. the frequency resolution of the Doppler spectrum is equal to $F_s/N_{FFT,DS}$. The total window size total window size $W_{FFT,DS}$ affects the reliability of the spectrum. To estimate the Doppler spread, the frequency at which the PSD drops by 3 dB relative to the maximum value is computed.

In this work, the algorithm to estimate the Doppler spread is evaluated assuming a rich scattering environment in which the multipath arrival is lumped into a signal bin arrival. The number of path arrivals is limited to 30 to respect the central limit theorem and create a circularly complex Gaussian fading channel.

The Doppler spread estimation algorithm is run for the frame defined in the Aquatron experiments. The Doppler spread is evaluated for increasing relative speeds between 0 and 30 knots. The sampling frequency is $Fs = 24$ kHz, and here we use $N_{FFT,DS} = 2,048$. The window size is tested for different frame lengths.

The results of the Doppler spread estimation algorithm are shown in Figure 4. Specifically, the Doppler spectrum is shown in Figure 4a, while the Doppler Spread estimate is shown in Figure 4b. As can be noted, the Doppler spread estimate becomes more reliable with longer window size. However, for some applications, a long discovery message is not affordable.

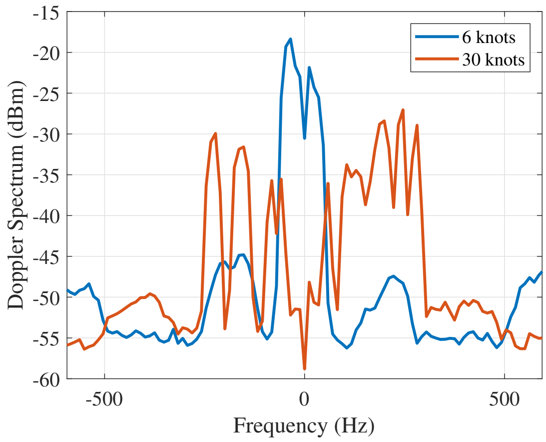

(a) Doppler spectrum for different relative speeds.

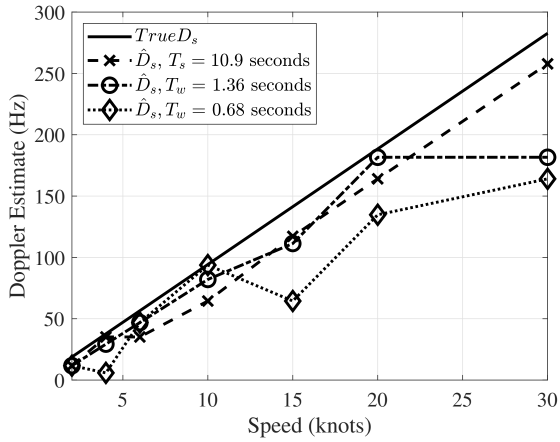

(b) Estimated Doppler spread vs. speed

Figure 4: Analysis of the Simulated Doppler Spread.

5. CONCLUSIONS

In this work, the use of a Janus-like discovery message to estimate different channel characteristics is described. The proposed estimator can be used to inform the nodes in the communication network to optimize the physical layer parameters as well as upper layer network settings. It is demonstrated that a figure of merit quantifying the channel multipath and Doppler spread can be fed back between the receiver and transmitter. For the multipath, it was demonstrated that the CFR variation of the estimated narrowband channel amplitudes over the bandwidth has a strong relationship with the RMS delay spread. A long message of 2048 symbols was used to acquire the statistics, and future work will investigate the impact of reducing the length. A Doppler spectrum can also be measured using a matched filter at the receiver, and the length of the window influences significantly the accuracy of the results. Specifically, it was shown that a window length longer than 1 second improves the accuracy of the Doppler spread estimation.

6. ACKNOWLEDGEMENTS

This research is funded by NSERC Discovery Grant #36263: ”Embedding Artificial Intelligence on Remote Underwater Sensor Nodes”.

REFERENCES

[1] Andreja Radosevic, Rameez Ahmed, Tolga M. Duman, John G. Proakis, and Milica Stojanovic. Adaptive OFDM Modulation for Underwater Acoustic Communications: Design Considerations and Experimental Results. *IEEE Journal of Oceanic Engineering*, 39(2):357–370, 2014.

[2] Linglong Dai, Zhaocheng Wang, Jun Wang, and Zhixing Yang. Joint Time-Frequency Channel Estimation for Time Domain Synchronous OFDM Systems. *IEEE Transactions on Broadcasting*, 59(1):168–173, 2013.

[3] Yifan Zhang, Jinhua Wang, Yaqing Huang, and Zhigang Gao. A Cooperative Approach for Adaptive Channel Discovery in Underwater Acoustic Communication. *Sensors*, 20(7):2012, 2020.

[4] Liang Wang, Yongqiang Yu, Kun Xie, Xuan Zhu, Guangjie Liu, Jiafeng Wang, and Hongming Zhang. Accurate Channel Estimation and Adaptive Underwater Acoustic Communications Based on Gaussian Likelihood and Constellation Aggregation. *Sensors (Basel, Switzerland)*, 22(6):2142–, 2022.

[5] Koen C.H. Blom, Henry S. Dol, Frank Berning, and Paul A. Van Walree. Development of a Physical Layer for Adaptive Underwater Acoustic Communications. In *2022 Sixth Underwater Communications and Networking Conference (UComms)*, pages 1–5, 2022.

[6] John Potter, João Alves, Dale Green, Giovanni Zappa, Ivor Nissen, and Kim McCoy. The JANUS underwater communications standard. In *2014 Underwater Communications and Networking (UComms)*, pages 1–4, 2014.

[7] Habib Mirhedayati Roudsari and Jean-Francois Bousquet. A Time-Varying Filter for Doppler Compensation Applied to Underwater Acoustic OFDM. *Sensors*, 19(1), 2019.